# Dopamine influences attentional rate modulation in Macaque posterior parietal cortex

Jochem van Kempen[1*], Christian Brandt[2], Claudia Distler[3], Mark A. Bellgrove[4], Alexander Thiele[1]

[1] Biosciences Institute, Newcastle University, NE1 7RU, Newcastle upon Tyne, United Kingdom.

[2] Institute of Clinical Research, University of Southern Denmark, 5230 Odense M, Denmark.

[3] Allgemeine Zoologie und Neurobiologie, Ruhr-Universität Bochum, 44801 Germany

[4] Turner Institute for Brain and Mental Health, School of Psychological Sciences, Monash University, Melbourne, Victoria 3800, Australia.

* Jochem.van-kempen@newcastle.ac.uk

## Conflict of interest statement

There are no conflicts of interest.

## Acknowledgements

Funded by Wellcome trust 093104 (JvK, AT), MRC MR/P013031/1 (JvK, AT). MAB is supported by a Senior Research Fellowship from the Australian National Health and Medical Research Council (NHMRC). Funded by strategic research partnership between Newcastle University and Monash University.

## Abstract

Selective attention facilitates the prioritization of task-relevant sensory inputs over those which are irrelevant. Although cognitive neuroscience has made great strides in understanding the neural substrates of attention, our understanding of its neuropharmacology is incomplete. Cholinergic and glutamatergic contributions have been demonstrated, but emerging evidence also suggests an important influence of dopamine (DA). DA has historically been investigated in the context of frontal/prefrontal function arguing that dopaminergic receptor density in the posterior/parietal cortex is sparse. However, this notion was derived from rodent data, whereas in primates DA innervation in parietal cortex matches that of many prefrontal areas. We recorded single- and multi-unit activity whilst iontophoretically administering dopaminergic agonists and antagonists to posterior parietal cortex of rhesus macaques engaged in a spatial attention task. Out of 88 neurons, 50 showed modulation of activity induced by drug administration. Dopamine inhibited firing rates across the population according to an inverted-U shaped dose-response curve. D1 receptor antagonists diminished firing rates in broad-spiking units according to a monotonically increasing function. Additionally, dopamine modulated attentional signals in broad, but not narrow-spiking cells. Finally, both drugs modulated the pupil light reflex. These data show that dopamine plays an important role in shaping neuronal responses and modulates attentional processing in macaque parietal cortex.

## Significance statement

Dopamine is critically involved in high-level cognitive functions, and dopaminergic dysfunctions pertain to ageing and neurological and psychiatric disorders. Most previous studies focused on dopaminergic effects on prefrontal activity or its role in basal ganglia

circuitry. The effects of dopamine in other brain areas such as parietal cortex, despite its well-established role in cognition and cognitive dysfunction, have largely been overlooked. This study is the first to show dopaminergic modulation of parietal activity in general, and specific to spatial attention in the non-human primate, revealing cell-type specific effects of dopamine on attentional modulation.

## Introduction

Selective attention refers to prioritization of behaviorally relevant, over irrelevant, sensory inputs. Convergent evidence from human neuropsychological, brain imaging and non-human primate studies shows that fronto-parietal networks are crucial for selective attention (Posner, 1990; Desimone and Duncan, 1995; Corbetta and Shulman, 2011). Neuromodulation of attention-related activity in these networks occurs at least in part via glutamatergic (Herrero et al., 2013) and cholinergic inputs (Warburton and Rusted, 1993; Levin and Simon, 1998; Nelson et al., 2005; Sarter et al., 2005; Parikh et al., 2007; Furey et al., 2008; Herrero et al., 2008; Dasilva et al., 2019). Multiple lines of evidence, however, also suggest dopaminergic modulation (Bellgrove and Mattingley, 2008; Noudoost and Moore, 2011a; Soltani et al., 2013; Thiele and Bellgrove, 2018). Here we sought to understand how dopamine applied to macaque posterior parietal cortex (PPC) modulates attention-related activity.

The functional significance of dopamine is well-established for a number of brain areas, including the frontal cortex (executive control) and basal ganglia (motor control). For these regions, substantial across-species similarities allowed the development of mechanistic models with clinical translational value for various disorders (e.g., Parkinson's disease, schizophrenia or attention deficit hyperactivity disorder (ADHD)) (Arnsten et al., 2012; Thiele and Bellgrove, 2018). Species differences with respect to dopaminergic innervation do

69 however exist for posterior cortical areas, including the PPC. Although sparse in rodents,
70 dopaminergic innervation of parietal areas in non-human primates is comparable in strength
71 and laminar distribution to prefrontal regions (Berger et al., 1991). Moreover, macaque PPC
72 has high densities of dopamine transporter (DAT) immunoreactive axons (Lewis et al., 2001).
73 These observations align with dense dopaminergic receptor expression in human PPC
74 (Caspers et al., 2013) and imaging studies of clinical disorders where medications targeting
75 dopamine receptors or transporters modulate parietal activity (Mehta et al., 2000). Given
76 these data and the clinical significance of PPC function, greater understanding of
77 dopaminergic effects in this region is warranted.

78 Selective attention relies heavily on PPC integrity and multiple lines of evidence suggest that
79 dopamine modulates attentional processes related to parietal function. First, dopamine
80 agonists reduce spatial inattention in neurological (Gorgoraptis et al., 2012) and psychiatric
81 patients with disorders such as schizophrenia (Maruff et al., 1995) and ADHD (Bellgrove et
82 al., 2008; Silk et al., 2014). Second, psychopharmacological studies in healthy volunteers
83 suggest that dopamine antagonists modulate parameters of spatial cueing paradigms (e.g.
84 validity effect), often associated with parietal function (Clark et al., 1989). Third, DNA
85 variation in a polymorphism of the dopamine transporter gene (DAT1) is associated with
86 individual differences in measures of spatial selective attention (Bellgrove et al., 2007, 2009;
87 Newman et al., 2014). Fourth, non-human primate studies revealed dopaminergic
88 contributions to working memory signals in dorsolateral prefrontal cortex (dlPFC) (Williams
89 and Goldman-Rakic, 1995), and modulation of dopaminergic signaling in frontal eye fields
90 (FEF) affects V4 neurons in a manner similar to attention and biases behavioral choices
91 (Noudoost and Moore, 2011a; Soltani et al., 2013). Dopamine thus contributes to working
92 memory, target selection and probably also spatial attention in dlPFC and FEF (Williams and
93 Goldman-Rakic, 1995; Noudoost and Moore, 2011a, 2011b; Clark and Noudoost, 2014).

Both areas are critical nodes of fronto-parietal attention networks. Thus, while dopaminergic influences on frontal circuits are comparatively well understood, their effect on attention-related activity in PPC is yet to be established.

Here we sought to address this knowledge gap by locally infusing dopamine or the selective D1 receptor (D1R) antagonist SCH23390 into the PPC of two macaque monkeys during a selective attention task. We show that single and multi-unit (SU, MU) activity is inhibited by iontophoresis of dopaminergic drugs into intraparietal sulcus (IPS) gray matter. The effects of the non-selective agonist dopamine (DA) followed an inverted U-shaped dose-response curve, whereas the D1-selective antagonist SCH23390 dose-response followed a monotonic function. Additionally, we found cell-type specific effects on attentional modulation whereby DA affected attention-related activity in broad but not narrow-spiking units. Finally, both drugs reduced the pupillary light reflex.

# Materials & Methods

## Procedures

All animal procedures were performed in accordance with the European Communities Council Directive RL 2010/63/EC, the National Institute of Health's Guidelines for the Care and Use of Animals for Experimental Procedures, and the UK Animals Scientific Procedures Act. Animals were motivated to engage in the task through fluid control at levels that do not affect animal physiology and have minimal impact on psychological wellbeing (Gray et al., 2016).

## Surgical preparation

The monkeys were implanted with a head post and recording chambers over the lateral intraparietal sulcus under sterile conditions and under general anesthesia. Surgery and postoperative care conditions have been described in detail previously (Thiele et al., 2006).

## Behavioral paradigms

Stimulus presentation and behavioral control was regulated by Remote Cortex 5.95 (Laboratory of Neuropsychology, National Institute for Mental Health, Bethesda, MD). Stimuli were presented on a cathode ray tube (CRT) monitor at 120 Hz, 1280 × 1024 pixels, at a distance of 54 cm.

The location of the saccade field (SF) was mapped using a visually guided saccade task. Here, monkeys fixated centrally for 400 ms after which a saccade target was presented in one of nine possible locations (8-10° from fixation, equally spaced between). After a random delay (800-1400 ms, uniformly distributed) the fixation point was extinguished, which indicated to the monkey to perform a saccade towards the target. Online analysis of visual, sustained and saccade related activity determined an approximate SF location which guided our subsequent receptive field (RF) mapping. The location and size of RFs were measured as described previously (Gieselmann and Thiele, 2008), using a reverse correlation method. Briefly, during fixation, a series of black squares (1-3° size, 100% contrast) were presented for 100 ms at pseudorandom locations on a 9 × 12 grid (5-25 repetitions for each location) on a bright background. RF eccentricity ranged from 2.5° to 17° and were largely confined to the contralateral visual field.

The main task and stimuli have been described previously (Thiele et al., 2016; van Kempen et al., 2020). In brief, stimuli were presented on a cathode ray tube (CRT) monitor (120 Hz,

1280 × 1024 pixels, 55 cm from the animal). The monkey initiated a trial by holding a lever and fixating a white fixation spot (0.1°) displayed on a grey background (1.41 cd/m$^2$). After 425/674 ms [monkey 1/monkey 2] three colored square wave gratings (2° - 6°, dependent on RF size and distance from fixation) appeared equidistant from the fixation spot, one of which was centered on the RF of the recorded neuron. Red, green and blue gratings (see Table 1 for color values) were presented with an orientation at a random angle to the vertical meridian (the same orientation for the three gratings in any given session). The locations of the colors, as well as the orientation, were pseudorandomly assigned between recording sessions and held constant for a given recording session. Gratings moved perpendicular to the orientation, whereby the direction of motion was pseudorandomly assigned for every trial. After a random delay (570-830/620-940 ms [monkey 1/monkey 2], uniformly distributed in 1 ms steps) a central cue appeared that matched the color of the grating that would be relevant on the current trial. After 980-1780/1160-1780 ms [monkey 1/monkey 2] (uniformly distributed in 1 ms steps), one pseudorandomly selected grating changed luminance (dimmed). If the cued grating dimmed, the monkey had to release the lever to obtain a reward. If a non-cued grating dimmed, the monkey had to ignore this and wait for the cued grating to dim. This could happen when the second or third grating changed luminance (each after 750-1130/800-1130 ms [monkey 1/monkey 2], uniformly distributed in 1 ms steps). Drugs were administered in blocks of 36 trials. The first block was always a control block. Thereafter, drug blocks and recovery blocks were alternated until the animal stopped working (number of block reversals, median ± interquartile range = 12 ± 6).

## Identification of recording sites

The location of the IPS was initially guided by means of postoperative structural magnetic resonance imaging (MRI), displaying the recording chamber. During each recording, neuronal response properties where determined using SF and RF mapping tasks. During the SF mapping task, we targeted cells that showed spatially selective persistent activity and preparatory activity before the execution of a saccadic eye movement.

## Electrode-pipette manufacturing

We recorded from the lateral (and in a few occasions medial) bank of the IPS using custom-made electrode-pipettes that allowed for simultaneous iontophoretic drug application and extracellular recording of spiking activity (Thiele et al., 2006). The location of the recording sites in one of the monkeys was verified in histological sections stained for cyto- and myeloarchitecture (Distler and Hoffmann, 2001) .

The manufacture of the electrodes was similar to the procedures described by Thiele et al., (2006), with minor changes to the design in order to reach areas deeper into the IPS, such as the ventral part of the lateral intraparietal area (LIPv). We sharpened tungsten wires (125 µm diameter, 75 mm length, Advent Research Materials Ltd., UK) by electrolytic etching off the tip (10-12 mm) in a solution of $NaNO_2$ (172.5 g), KOH (85 g) and distilled water (375 ml). We used borosilicate glass capillaries with three barrels (custom ordered, Hilgenberg GmBH, www.hilgenberg-gmbh.de), with the same dimensions as those described previously (Thiele et al., 2006). The sharpened tungsten wire was placed in the central capillary and secured in place by bending the non-sharpened end (approximately 10 mm) of the wire over the end of the barrel. After marking the location of the tip of the tungsten wire, shrink tubing was placed around the top and bottom of the glass. The glass was pulled around the tungsten wire using a

186 PE-21 Narishige microelectrode puller with a heating coil made from Kanthal wire (1 mm
187 diameter, 13 loops, inner loop diameter 3 mm) and the main (sub) magnet set to 30 (0) and
188 the heater at 100. The electrode-pipette was placed such that the tip of the tungsten wire
189 protruded 11 mm from the bottom of the heating coil. After pulling, we filled the central
190 barrel (with the tungsten electrode inside) with superglue using a syringe and fine flexible
191 injection cannula (MicroFil 28 AWG, MF28G67-5, World Precision Instruments, Ltd.). We
192 found that if we did not fill (most of) the central barrel with superglue after pulling, the
193 recorded signal was often very noisy, possibly due to small movements of the animal (such as
194 drinking), which caused the free tungsten wire to resonate inside the glass. Using a micro
195 grinder (Narishige EG-400), we removed excess glass, sharpened the tip of the electrode and
196 opened the flanking barrels of the pipette. This pulling procedure resulted in a pulled
197 electrode part of approximately 2.5 cm length, with gradually increasing diameter, from ~10
198 µm to ~200 µm, over the first 12 mm of the electrode-pipette.

199

200 ## Electrode-pipette filling and iontophoresis

201 Electrode-pipettes were back-filled with the same drug in both pipettes using a syringe, filter
202 units (Millex® GV, 22 µm pore diameter, Millipore Corporation) and fine flexible injection
203 cannula (MicroFil 34 AWG, MF34G-5, World Precision Instruments, Ltd.). The pipettes
204 were connected to the iontophoresis unit (Neurophore-BH- 2, Medical systems USA) with
205 tungsten wires (125 µm diameter) inserted into the flanking barrels. Because of the
206 exploratory nature of these recordings (it is unknown whether DA influences parietal neurons
207 during spatial attention tasks and what modulation can be expected with different amounts of
208 drug applied), we used a variety of iontophoretic ejection currents (20 - 90 nA). The details

regarding concentration and pH of the drugs were: Dopamine (0.1M in water for injections, pH 4-5) and SCH23390 (0.005-0.1M in water for injections, pH 4-5).

## Data acquisition

Stimulus presentation, behavioral control and drug administration was regulated by Remote Cortex 5.95 (Laboratory of Neuropsychology, National Institute for Mental Health, Bethesda, MD). Raw data were collected using Remote Cortex 5.95 (1-kHz sampling rate) and by Cheetah data acquisition (32.7-kHz sampling rate, 24-bit sampling resolution) interlinked with Remote Cortex 5.95. Data were replayed offline, sampled with 16-bit resolution and band-pass filtered (0.6-9 kHz). Spikes were sorted manually using SpikeSort3D (Neuralynx). Eye position and pupil diameter were recorded using a ViewPoint eyetracker (Arrington research) at 220 Hz. Pupil diameter was recorded in 40 out of 54 recording sessions.

## Pupillometry

Pupil diameter was low pass filtered (10 Hz) using a second order Butterworth filter. Baseline activity was estimated as the average activity before stimulus onset (-300 to -50 ms), which was used to normalize the pupil diameter time course. Stimulus evoked pupil constriction was baseline corrected (on a trial by trial basis) and averaged in a 250 ms time window centered on 500 ms after stimulus onset. Cue-evoked (250 ms window centered on 500 ms after cue onset) and pre-dimming (-300 to -50 ms) pupil diameter, was baseline subtracted with a pre-cue baseline (-300 to -50 ms). For visualization, pupil diameter in each epoch was scaled to a range from zero to one, before averaging across trials.

## Analysis of cell type.

We distinguished between different cell types based on the duration of the extracellular spike waveform as described in Thiele et al. (2016). Specifically, we classified cells based on the peak-to-trough ratio, i.e. the duration between the peak and the trough of the interpolated (cubic spline) spike waveform. To test whether the distribution of peak-to-trough distance of the spike waveforms was unimodal (null hypothesis) or bimodal, indicating that our distribution contained different cell types, a modified Hartigan's dip test was used (Ardid et al., 2015; Thiele et al., 2016). We used a cut-off of 250 µs to classify cells as narrow or broad spiking, as this was where our distribution revealed the main 'dip' (Figure 3A-B).

## Fano factor

The variability of neural responses was quantified using Fano factors ($FF$), computed as the ratio between the variance ($\sigma^2$) and the mean ($\mu$) spike counts within the time window of interest, defined as:

$$FF = \frac{\sigma^2}{\mu}$$

## Drug modulation

The strength of the effect of drug application on neural activity (firing rates) was determined via a drug modulation index ($drugMI$), defined as:

$$drugMI = \frac{drug_{on} - drug_{off}}{drug_{on} + drug_{off}}$$

with $drug_{on}$ as the neural activity when drug was applied, and $drug_{off}$ the activity when the drug was not applied. This index ranges from -1 to 1, with zero indicating no modulation due

to drug application and with positive values indicating higher activity when the drug was applied and conversely, negative values indicating lower activity.

## Quantification of attentional rate modulation.

To quantify the difference between neural responses when attention was directed towards the RF versus away from the RF, we computed the area under the receiver operating characteristic (AUROC) curve. Stemming from signal detection theory (Green and Swets, 1966), this measure represents the difference between two distributions as a single scalar value, taking into account both the average difference in magnitude as well as the variability of each distribution. This value indicates how well an ideal observer would be able to distinguish between two distributions, for example the neural response when attention is directed towards versus away from its RF. It is computed by iteratively increasing the threshold and computing the proportion (from the first sample to the threshold) of hits and false alarms (FA), i.e. the correct and false classification as samples belonging to one of the activity distributions. The ROC curve is generated by plotting the proportions of hits against the proportion of FAs, and AUROC is taken as the area under the ROC curve. An AUROC of 0.5 indicates that the two distributions were indistinguishable, whereas an AUROC of 0 or 1 indicates that the two distributions were perfectly separable.

## Experimental design and statistical analysis

We recorded single (SU, n=40) and multi-unit (MU, n=48) activity (total 88 units; 64 from monkey 1, 24 from monkey 2) from 2 male rhesus macaque monkeys (*Macaca mulatta,* age 9-11 years, weight 8-12.9 kg).

To determine whether DA significantly affected neural activity across the population of units, we used two-sided paired-sample Wilcoxon signed rank tests. For comparisons within one recording, e.g. spike rates across trials for different conditions, we used analysis of variance (ANOVA) with three factors: attention (towards or away from the RF), drug (on or off) and stimulus direction. To test whether drug application affected behavioral performance, we used sequential linear mixed effects models with attention and drug as fixed effects and with the recording number as a random effect, to account for the repeated measurements in the data.

To test for significant linear or quadratic trends in the drug dose-response curve, we used sequential linear mixed effects models and likelihood ratio tests. Specifically, we tested whether a first order (linear) polynomial fit was better than a constant (intercept-only) fit and subsequently whether a second order (non-monotonic) polynomial fit was better than a linear fit. The modulation due to drug application of the neural response $y$ was modelled as a linear combination of polynomial basis functions of the iontophoretic ejection current ($X$):

$$y \sim \beta_0 + \beta_1 X + \beta_2 X^2$$

, with $\beta$ as the polynomial coefficients. When a significant quadratic relationship was found, we used the two-lines approach to determine whether this relationship was significantly U-shaped (Simonsohn, 2017). Error bars in all figures indicate the standard error of the mean (SEM), unless stated otherwise.

We selected which cells to include in each of the analyses based on the output of the 3-factor ANOVA described above. For example, if we wanted to investigate whether drug application affected attentional modulation of firing rates, we only included cells that revealed a main or interaction effect for both attention and drug application.

## Code

Data analyses were performed using custom written scripts in Matlab (the Mathworks) and RStudio (RStudio Team (2016). RStudio: Integrated Development for R. RStudio, Inc., Boston, MA URL http://www.rstudio.com). Data and analysis scripts necessary to reproduce these results are available upon reasonable request.

# Results

We recorded activity from 88 single and multi-units from intraparietal sulcus (IPS) in two awake, behaving Macaque monkeys performing a selective attention task (Figure 1A). Of these cells, 86 (97.7%) showed a visual response to stimulus onset and 74 (84.1%) were modulated by attention (Figure 1B). During recording, we used an electrode-pipette combination to iontophoretically administer dopaminergic (DA) drugs in the vicinity of the recorded cells (Thiele et al., 2006). Across the two monkeys, we recorded from 59 units whilst administering the unselective agonist dopamine and from 29 units during which we administered the selective D1R antagonist SCH23390. Firing rates in 36 (61%) and 14 (48.3%) units were modulated by application of the unselective agonist dopamine and SCH23390, respectively (Figure 1B). Thus, around half the units were modulated both by attention and drug application (Figure 1B), which is comparable to cholinergic modulation of attention induced activity in macaque V1 and FEF (Herrero et al., 2008; Dasilva et al., 2019).

Figure 2A illustrates the population activity (from all units) aligned to stimulus onset, cue onset and the first-dimming event, for both the no-drug and the drug conditions. For a given drug condition, neural activity between attention conditions did not differ when aligned to stimulus onset but started to diverge approximately 200 ms after cue onset, indicating which of the three gratings was behaviorally relevant on that trial, and diverged further leading up to

325 the first dimming event. Across the population, dopamine strongly reduced firing rates
326 throughout the duration of the trial, including during baseline periods as well as stimulus and
327 cue presentation. The effects of SCH23390 were of the same sign but weaker. Although drug
328 induced changes to attentional modulation of neural activity appear relatively small at the
329 population level (using visual inspection, compare the difference between the dark and light
330 blue lines and the difference between the red and orange lines), a subset of neurons revealed
331 an interaction between attention and drug application (Figure 1B), as illustrated for an
332 example neuron in Figure 2B, and these effects depended on the cell types affected (see
333 below). Next, we specifically examined units that were modulated by attention and/or drug
334 application and investigated whether activity modulation due to attention and drug
335 application mapped onto different cell types.

336 Cells were classified as narrow or broad-spiking cells according to the median duration of the
337 peak-to-trough time of the spike waveforms (Figure 3A & B). These cell types have
338 previously been found to respond differently to dopaminergic drug application (Jacob et al.,
339 2013, 2016). Although narrow and broad-spiking cells have been argued to respectively
340 constitute inhibitory interneurons and excitatory pyramidal cells (Mitchell et al., 2007), a
341 more recent study found that output cells in primary motor cortex (unequivocal pyramidal
342 cells) had a narrow action potential waveform (Vigneswaran et al., 2011), and most
343 pyramidal cells in macaque PFC express the Kv3.1b potassium channel, associated with the
344 generation of narrow spikes (Soares et al., 2017). Therefore, the narrow-broad categorization
345 solely allows to distinguish between 2 different cell-type categories, without mapping this
346 classification specifically onto interneurons or pyramidal cells, let alone a more fine-grained
347 distinction.

348 The application of DA reduced firing rates across the population of both broad and narrow
349 spiking units, and for both the attend towards and away from RF conditions (Figure 3C).

350 Fano factors were unaffected by dopamine application (Figure 3D). The application of
351 SCH23390 elicited a small but significant reduction of the average firing rates of broad-
352 spiking units during both attention conditions (Figure 3E) without affecting FFs (Figure 3F).
353 Dopaminergic drug application thus mainly inhibited cellular activity, without affecting the
354 rate variability, as quantified by FFs.

355 To investigate whether dopamine affected attention-specific activity, we tested whether
356 attention AUROC values were modulated by drug application. Attention AUROC values
357 indicate how well an ideal observer can distinguish between neural activity during attend RF
358 or attend away trials. A value of 0.5 indicates that the distributions are indistinguishable,
359 whereas values of 0 or 1 indicate perfectly distinguishable distributions. The application of
360 the non-specific agonist dopamine reduced AUROC values for broad-spiking cells, whereas
361 narrow-spiking cells were unaffected (Figure 4A). SCH23390 application did not modulate
362 AUROC values for either cell type (Figure 4B). Dopamine thus had a cell-type specific effect
363 on attentional rate modulation.

364 We applied dopaminergic drugs with a variety of iontophoretic ejection currents (20-90 nA).
365 Since dopamine has previously been shown to modulate neural activity according to an
366 inverted U-shaped dose-response curve (Vijayraghavan et al., 2007), with maximal
367 modulation at intermediate dopamine levels, we tested whether the ejection current was
368 predictive of the firing rate modulation associated with drug application, estimated by a drug
369 modulation index (drugMI). Specifically, we used sequential linear mixed effects model
370 analyses and likelihood ratio tests to test for linear and quadratic trends. U-shaped trends
371 were verified using the two-lines approach (Materials & Methods). The non-specific agonist
372 dopamine displayed a non-monotonic relationship with drugMI ($\chi^2_{(1)} = 7.18$, $p = 0.007$) and
373 revealed an inverted U-shaped curve ($p < 0.05$) in which intermediate ejection currents
374 elicited the most negative drugMI, i.e. the largest inhibition of activity (Figure 4C). For

375 SCH23390, on the other hand, we found a monotonic dose-response relationship ($\chi^2_{(1)} = 4.21$,
376 $p = 0.040$), with more inhibition of firing rates with higher drug ejection currents (Figure
377 4D). To investigate whether drug dosage was also predictive of attentional rate modulation,
378 we performed the same analysis on the difference score (drug – no drug) of attention
379 AUROC values. Neither dopamine ($\chi^2_{(1)} = 0.95$, $p = 0.330$), nor SCH23390 ($\chi^2_{(1)} = 0.33$, $p =$
380 $0.568$) dosage were predictive of attention AUROC (data not shown). Comparable results
381 were obtained when these analyses were limited to only broad spiking cells, or cells that
382 showed both an attention and drug effect.

383 As drug application strongly inhibited firing rates across the population and we found cell-
384 type specific effects on attention-specific activity, we next investigated whether drug
385 application affected behavioral performance (Figure 5). To this end, we used sequential
386 multilevel model analyses to test for fixed effects of attention and drug application, as well as
387 their interaction, on RT. Neither attention (Dopamine: $\beta = -13.49 \pm 8.88$, $p = 0.132$;
388 SCH23390: $\beta = 2.86 \pm 11.34$, $p = 0.802$), nor drug application (Dopamine: $\beta = -3.47 \pm 8.88$, $p =$
389 $0.697$; SCH23390: $\beta = 10.38 \pm 11.34$, $p = 0.363$) nor their interaction (Dopamine: $\beta =$
390 $2.87 \pm 5.62$, $p = 0.611$; SCH23390: $\beta = -4.33 \pm 7.17$, $p = 0.548$) were predictive of RT for either
391 drug. Given the focal nature of micro-iontophoretic drug application (Herz et al., 1969), the
392 absence of an effect of drug application on behavioral performance is not surprising and in-
393 line with comparable work on DA in PFC (Vijayraghavan et al., 2007; Jacob et al., 2013,
394 2016).

395 Interestingly, however, we found that the application of both DA and SCH23390 influenced
396 pupil diameter. We conducted a sliding-window Wilcoxon signed rank analysis for each 200
397 ms window, in 10 ms increments, comparing baseline-normalized pupil diameter on drug
398 compared to no-drug trials (Figure 6A). This analysis revealed a significant difference in
399 pupil diameter that started after stimulus onset and lasted until after cue onset. Specifically,

400 we found a small, but significant, modulation of the pupillary light reflex (Figure 6). The
401 magnitude of the constriction of the pupil upon stimulus onset was reduced during
402 dopaminergic drug application compared to control trials, but neither drug influenced pupil
403 diameter during any other time window (Figure 6B-E). Another sliding window analysis
404 using a two factor (drug by attention) repeated measures ANOVA revealed no effect of
405 attention (main or interaction) on pupil diameter (data not shown). Thus, locally applied
406 dopaminergic drugs in parietal cortex modulated the pupillary light reflex.

407

## 408 Discussion

409 We tested the effects of dopaminergic drugs on PPC activity during spatial selective
410 attention. The non-specific agonist dopamine inhibited activity according to an inverted U-
411 shaped dose-response curve, whereas the D1R antagonist decreased firing rates for broad-
412 spiking units following a monotonic dose-response curve. Dopamine additionally reduced
413 attention-related firing rate modulations in broad-spiking units. Finally, local drug application
414 in parietal cortex decreased the pupillary light reflex. This is the first study (to the best of our
415 knowledge) revealing the role of dopaminergic modulation on attention-related activity in
416 parietal cortex.

417

### 418 General and cell-type specific dopaminergic modulation in parietal cortex

419 We distinguished between broad and narrow-spiking units. Even though, as discussed above,
420 this classification does not reflect a one-to-one mapping onto interneurons and pyramidal
421 cells, this categorization may explain some of our results (Jacob et al., 2013, 2016).
422 Dopamine has a well-established role in modulating prefrontal signaling, supporting

423 cognitive functions such as working memory and attention (Williams and Goldman-Rakic,
424 1995; Watanabe et al., 1997; Vijayraghavan et al., 2007; Noudoost and Moore, 2011b; Clark
425 and Noudoost, 2014; Thiele and Bellgrove, 2018; Ott and Nieder, 2019). D1R and D2R are
426 expressed broadly throughout the cortex and fulfil complementary roles in prefrontal
427 cognitive control (Ott and Nieder, 2019). Although D2Rs have been implicated in rule coding
428 (Ott et al., 2014), modulation of working memory is mostly associated with D1R stimulation
429 or blockade (Sawaguchi et al., 1990; Sawaguchi and Goldman-Rakic, 1991, 1994; Williams
430 and Goldman-Rakic, 1995). Moreover, while manipulation of either receptor subtype in FEF
431 can modulate behavioral choices (Soltani et al., 2013), only D1R blockade in FEF elicited
432 activity resembling attentional effects in extrastriate visual areas (Noudoost and Moore,
433 2011a). Interestingly, D1R expression is higher in FEF pyramidal cells compared to
434 interneurons (Mueller et al., 2018, 2019). Here, dopaminergic drugs affected broad-spiking
435 more than narrow-spiking units. Although it is unknown whether dopamine receptor
436 expression differs across cell types in PPC, if expression is similar to the FEF, modulation of
437 parietal attentional signals might rely on higher expression of D1R compared to D2R in
438 broad-spiking putative pyramidal cells.

439 It is remarkable that the majority of the recorded neurons were inhibited by dopamine and
440 SCH23390 application, as previous studies (in prefrontal cortex) found mixed responses to
441 unselective dopamine (Jacob et al., 2013) or D1R stimulation (Williams and Goldman-Rakic,
442 1995; Vijayraghavan et al., 2007). These effects could theoretically be due to our
443 recording/iontophoresis setup. As both agonists and antagonists elicited responses of the
444 same sign, effects unrelated to specific drugs could have been ruled out by control recordings
445 using saline or by compensating ejection currents. Similar control experiments from our lab
446 (and other labs) have, however, never resulted in systematic (condition specific) effects
447 (Herrero et al., 2008, 2013, 2017; Thiele et al., 2012; Jacob et al., 2013; Ott et al., 2014; Ott

448 and Nieder, 2016; Dasilva et al., 2019). Further, the cell-type specific effects and U-shaped
449 dose-response curve argue against our results being an iontophoresis artefact.

450 These effects may alternatively be explained by drug dosages. Although Jacob et al. (2013)
451 used a variety of ejection currents (25-100 nA) and the proportion of inhibited or excited cells
452 did not differ by dosage, activity increases have been found for low, and decreases for high
453 D1R-agonist and antagonist dosages (Williams and Goldman-Rakic, 1995; Vijayraghavan et
454 al., 2007). Indeed, while our sample size using lower dosages was small, lower ejection
455 currents predicted positive and less negative modulation. At the dosages used in this study,
456 dopamine could have mostly inhibitory effects. Vijayraghavan et al. (2007) found that low
457 doses (10-20 nA) of D1-agonists reduced overall firing rates, but increased spatial specificity
458 of prefrontal neurons, whereas high dosages (20-100 nA) further reduced activity and
459 abolished spatially selective information. Given that our study was unrelated to spatial
460 specificity (i.e. saccade field tuning), we were unable to assess this particular feature, but
461 dopaminergic influences may still enhance spatial tuning of PPC despite an overall reduction
462 in activity.

463 Another factor that could explain the low number of dopamine-excited units is the short
464 block duration used in our task. Cells excited by dopamine respond slower to drug
465 application than inhibited cells, with an average modulation up-ramp time constant of 221.9 s
466 (Jacob et al., 2013). In our task, with a median trial duration of approximately 8 s, a block (36
467 trials) lasted approximately 288 s. Dopamine-excited neurons could have only started to show
468 modulation towards the end of the block, resulting in a population of largely inhibited units.

469 In sum, dopaminergic effects on (task-related) activity are complex (Seamans and Yang,
470 2004) and depend on various factors not controlled for in this study, such as endogenous
471 levels of dopamine. Within prefrontal cortex, coding can be enhanced by D1R agonists, and

472 diminished by antagonists (Vijayraghavan et al., 2007; Ott et al., 2014), or vice-versa
473 (Williams and Goldman-Rakic, 1995; Noudoost and Moore, 2011a). Indeed, dopaminergic
474 effects show regional variability across different brain areas, even within PFC (Arnsten et al.,
475 2012). Thus, the mechanisms discussed above might not apply to PPC. Future studies are
476 needed to further elucidate cell-type and receptor-subtype specific effects of dopamine in
477 parietal cortex during task performance.

478

479 ## Dopaminergic dose-response curve

480 Dopamine receptor stimulation follows an inverted-U shaped dose-response curve whereby
481 too little or too much stimulation leads to suboptimal behavioral performance (Arnsten et al.,
482 1994; Zahrt et al., 1997) or neural coding (Vijayraghavan et al., 2007). Whereas optimal
483 levels of dopamine receptor stimulation can stabilize and tune neural activity, suboptimal
484 levels decrease neural coding and behavioral performance.

485 Here we found an inverted-U shaped dose-response curve for the unselective agonist
486 dopamine, and a monotonic function for the D1R antagonist SCH23390. Rather than
487 predicting neural coding for attention, however, ejection currents were merely predictive of
488 drug modulation indices, without any relationship to attention AUROC values. However, our
489 sample size, especially for SCH23390, might have been too small to reliably determine the
490 shape of the dose-response curve. Additionally, the dopaminergic effects might partly be
491 driven by receptor subtypes (e.g. D2R) not usually associated with modulation of delay
492 period activity. While this study provides evidence for a role of dopamine in parietal cortex
493 during cognitive tasks, further research is required to elucidate the exact underlying
494 mechanisms.

495

496 ## Dopaminergic modulation of the pupil light reflex

497 The pupil light reflex (PLR) transiently constricts the pupil after exposure to increases in
498 illumination or presentation of bright stimuli (Loewenfeld, 1993; McDougal and Gamlin,
499 2014). Recent studies have shown that covert attention can modulate this behavioral reflex
500 (Naber et al., 2013; Binda and Murray, 2015a, 2015b). Subthreshold FEF microstimulation
501 respectively enhances or reduces the PLR when a light stimulus is presented inside or outside
502 the saccade field (Ebitz and Moore, 2017). The PLR thus depends both on luminance changes
503 and the location of spatial attention. We found that dopaminergic drug application in parietal
504 cortex reduced the PLR. These results are in agreement with the electrophysiological results,
505 as drug administration also reduced attentional rate modulation. Two (non-exclusive)
506 mechanisms have been proposed by which FEF can modulate the PLR (Binda and Gamlin,
507 2017). By direct or indirect projections to the olivary pretectal nucleus, or via indirect
508 projections to constrictor neurons in the Edinger-Westphal nucleus. For the latter, these
509 projections are hypothesized to pass through extrastriate visual cortex and/or the superior
510 colliculus (SC). Subthreshold microstimulation of the intermediate (SCi), but not superficial
511 (SCs), layers of the SC elicits a short latency pupillary dilation (Wang et al., 2012; Joshi et
512 al., 2016). Whereas the SCs receives input from early visual areas, including the retina, the
513 SCi receives input from higher-order association cortices. Along with preparing and
514 executing eye movements, the SCi is involved in directing covert attention (Kustov and Lee
515 Robinson, 1996; Ignashchenkova et al., 2004; Muller et al., 2005; Lovejoy and Krauzlis,
516 2010), and provides an essential contribution to the selection of stimuli amongst competing
517 distractors (McPeek and Keller, 2002, 2004; reviewed in Mysore and Knudsen, 2011).
518 Moreover, the SC receives dense projections from parietal cortex (Kuypers and Lawrence,
519 1967; Becker, 1989), and has been hypothesized to play an important role in pupil diameter
520 modulation (Wang and Munoz, 2015). It is currently unclear whether dopaminergic

521 modulation of frontal (or parietal) cortex modulates SC activity, but this pathway seems a
522 strong candidate for the modulation of the PLR (Wang and Munoz, 2015) that we
523 encountered in this study through DA application.

524 Dopamine is an important modulator of high-level cognitive functions, both in the healthy
525 and ageing brain as well as for various clinical disorders (Robbins and Arnsten, 2009;
526 Arnsten et al., 2012; Thiele and Bellgrove, 2018). Although dopaminergic effects within PFC
527 have been elucidated in some detail, the effects of dopamine in other brain areas such as
528 parietal cortex, despite its well-established role in cognition and cognitive dysfunction, has
529 largely been overlooked. This study is the first to show dopaminergic modulation of parietal
530 activity in general, and activity specific to spatial attention in the non-human primate. Our
531 work encourages future studies of dopaminergic involvement in parietal cortex, thereby
532 gaining a broader understanding of neuromodulation in different networks for cognition.

533

534 ## References


535 Ardid S, Vinck M, Kaping D, Marquez S, Everling S, Womelsdorf T (2015) Mapping of
536 functionally characterized cell classes onto canonical circuit operations in primate
537 prefrontal cortex. J Neurosci.

538 Arnsten AFT, Cai JX, Murphy BL, Goldman-Rakic PS (1994) Dopamine D1 receptor
539 mechanisms in the cognitive performance of young adult and aged monkeys.
540 Psychopharmacology (Berl).

541 Arnsten AFT, Wang MJ, Paspalas CD (2012) Neuromodulation of Thought: Flexibilities and
542 Vulnerabilities in Prefrontal Cortical Network Synapses. Neuron 76:223–239.

543 Becker W (1989) The neurobiology of saccadic eye movements. Metrics. Rev Oculomot Res
544 3:13–67 Available at: http://www.ncbi.nlm.nih.gov/pubmed/2486323.

545 Bellgrove MA, Barry E, Johnson KA, Cox M, Dáibhis A, Daly M, Hawi Z, Lambert D,
546 Fitzgerald M, McNicholas F, Robertson IH, Gill M, Kirley A (2008) Spatial attentional
547 bias as a marker of genetic risk, symptom severity, and stimulant response in ADHD.
548 Neuropsychopharmacology 33:2536–2545.

549 Bellgrove MA, Chambers CD, Johnson KA, Daibhis A, Daly M, Hawi Z, Lambert D, Gill M,
550 Robertson IH (2007) Dopaminergic genotype biases spatial attention in healthy children.
551 Mol Psychiatry 12:786–792.

552 Bellgrove MA, Johnson KA, Barry E, Mulligan A, Hawi Z, Gill M, Robertson I, Chambers
553 CD (2009) Dopaminergic Haplotype as a Predictor of Spatial Inattention in Children
554 With Attention-Deficit/Hyperactivity Disorder. Arch Gen Psychiatry 66:1135 Available
555 at:
556 http://archpsyc.jamanetwork.com/article.aspx?doi=10.1001/archgenpsychiatry.2009.120

557 .

558 Bellgrove MA, Mattingley JB (2008) Molecular genetics of attention. In: Annals of the New
559 York Academy of Sciences, pp 200–212.

560 Berger B, Gaspar P, Verney C (1991) Dopaminergic innervation of the cerebral cortex:
561 Unexpected differences between rodents and primates. Trends Neurosci 14:21–27
562 Available at: http://linkinghub.elsevier.com/retrieve/pii/016622369190179X [Accessed
563 January 14, 2015].

564 Binda P, Gamlin PD (2017) Renewed Attention on the Pupil Light Reflex. Trends Neurosci
565 40:455–457 Available at: http://www.cell.com/trends/neurosciences/pdf/S0166-
566 2236(17)30122-4.pdf [Accessed July 26, 2017].

567 Binda P, Murray SO (2015a) Spatial attention increases the pupillary response to light
568 changes. J Vis 15:1–1.

569 Binda P, Murray SO (2015b) Keeping a large-pupilled eye on high-level visual processing.
570 Trends Cogn Sci 19:1–3 Available at: http://dx.doi.org/10.1016/j.tics.2014.11.002.

571 Caspers S, Schleicher A, Bacha-Trams M, Palomero-Gallagher N, Amunts K, Zilles K (2013)
572 Organization of the human inferior parietal lobule based on receptor architectonics.
573 Cereb Cortex 23:615–628.

574 Clark CR, Geffen GM, Geffen LB (1989) Catecholamines and the covert orientation of
575 attention in humans. Neuropsychologia 27:131–139.

576 Clark KL, Noudoost B (2014) The role of prefrontal catecholamines in attention and working
577 memory. Front Neural Circuits 8:33 Available at:
578 http://www.pubmedcentral.nih.gov/articlerender.fcgi?artid=3986539&tool=pmcentrez&
579 rendertype=abstract [Accessed November 5, 2014].

580 Corbetta M, Shulman GL (2011) Spatial Neglect and Attention Networks. Annu Rev
581 Neurosci 34:569–599 Available at:
582 http://www.annualreviews.org/doi/abs/10.1146/annurev-neuro-061010-113731.

583 Dasilva M, Brandt C, Gotthardt S, Gieselmann MA, Distler C, Thiele A (2019) Cell class-
584 specific modulation of attentional signals by acetylcholine in macaque frontal eye field.
585 Proc Natl Acad Sci:201905413 Available at:
586 http://www.pnas.org/lookup/doi/10.1073/pnas.1905413116.

587 Desimone R, Duncan J (1995) Neural Mechanisms of Selective Visual Attention. Annu Rev
588 Neurosci 18:193–222 Available at:
589 http://www.annualreviews.org/doi/abs/10.1146/annurev.ne.18.030195.001205.

590 Distler C, Hoffmann K-P (2001) Cortical Input to the Nucleus of the Optic Tract and Dorsal
591 Terminal Nucleus (NOT-DTN) in Macaques: a Retrograde Tracing Study. Cereb Cortex
592 11:572–580 Available at: https://academic.oup.com/cercor/article-
593 lookup/doi/10.1093/cercor/11.6.572.

594 Ebitz RB, Moore T (2017) Selective Modulation of the Pupil Light Reflex by
595 Microstimulation of Prefrontal Cortex. J Neurosci 37:5008–5018 Available at:
596 http://www.jneurosci.org/content/jneuro/early/2017/04/21/JNEUROSCI.2433-
597 16.2017.full.pdf [Accessed April 24, 2017].

598 Furey ML, Pietrini P, Haxby J V., Drevets WC (2008) Selective effects of cholinergic
599 modulation on task performance during selective attention. Neuropsychopharmacology.

600 Gieselmann MA, Thiele A (2008) Comparison of spatial integration and surround
601 suppression characteristics in spiking activity and the local field potential in macaque
602 V1. Eur J Neurosci 28:447–459.

603 Gorgoraptis N, Mah YH, MacHner B, Singh-Curry V, Malhotra P, Hadji-Michael M, Cohen
604 D, Simister R, Nair A, Kulinskaya E, Ward N, Greenwood R, Husain M (2012) The
605 effects of the dopamine agonist rotigotine on hemispatial neglect following stroke. Brain
606 135:2478–2491.

607 Gray H, Bertrand H, Mindus C, Flecknell P, Rowe C, Thiele A (2016) Physiological,
608 Behavioral, and Scientific Impact of Different Fluid Control Protocols in the Rhesus
609 Macaque (Macaca mulatta). Eneuro 3:1–15.

610 Green DM, Swets JA (1966) Signal Detection Theory and Psychophysics. New York: Wiley.

611 Herrero JL, Gieselmann M a, Sanayei M, Thiele A (2013) Attention-induced variance and
612 noise correlation reduction in macaque v1 is mediated by NMDA receptors. Neuron
613 78:729–739 Available at:
614 http://www.pubmedcentral.nih.gov/articlerender.fcgi?artid=3748348&tool=pmcentrez&
615 rendertype=abstract [Accessed January 6, 2015].

616 Herrero JL, Gieselmann MA, Thiele A (2017) Muscarinic and Nicotinic Contribution to
617 Contrast Sensitivity of Macaque Area V1 Neurons. Front Neural Circuits 11:1–15.

618 Herrero JL, Roberts MJ, Delicato LS, Gieselmann MA, Dayan P, Thiele A (2008)
619 Acetylcholine contributes through muscarinic receptors to attentional modulation in V1.
620 Nature 454:1110–1114 Available at:
621 http://www.pubmedcentral.nih.gov/articlerender.fcgi?artid=2666819&tool=pmcentrez&
622 rendertype=abstract [Accessed October 7, 2014].

623 Herz A, Zieglgänsberger W, Färber G (1969) Microelectrophoretic studies concerning the
624 spread of glutamic acid and GABA in brain tissue. Exp Brain Res 9 Available at:
625 http://link.springer.com/10.1007/BF00234456.

626 Ignashchenkova A, Dicke PW, Haarmeier T, Thier P (2004) Neuron-specific contribution of
627 the superior colliculus to overt and covert shifts of attention. Nat Neurosci 7:56–64
628 Available at: http://www.nature.com/articles/nn1169.

629 Jacob SN, Ott T, Nieder A (2013) Dopamine regulates two classes of primate prefrontal
630 neurons that represent sensory signals. J Neurosci 33:13724–13734 Available at:
631 http://www.ncbi.nlm.nih.gov/pubmed/23966694 [Accessed November 24, 2014].

632 Jacob SN, Stalter M, Nieder A (2016) Cell-type-specific modulation of targets and distractors
633 by dopamine D1 receptors in primate prefrontal cortex. Nat Commun.

634 Joshi S, Li Y, Kalwani RM, Gold JI (2016) Relationships between Pupil Diameter and
635 Neuronal Activity in the Locus Coeruleus, Colliculi, and Cingulate Cortex. Neuron
636 89:221–234 Available at: http://dx.doi.org/10.1016/j.neuron.2015.11.028.

637 Kustov AA, Lee Robinson D (1996) Shared neural control of attentional shifts and eye
638 movements. Nature 384:74–77 Available at: http://www.nature.com/articles/384074a0.

639 Kuypers HGJM, Lawrence DG (1967) Cortical projections to the red nucleus and the brain
640 stem in the rhesus monkey. Brain Res 4:151–188 Available at:
641 http://dx.doi.org/10.1016/j.brainres.2016.01.006.

642 Levin ED, Simon BB (1998) Nicotinic acetylcholine involvement in cognitive function in
643 animals. Psychopharmacology (Berl) 138:217–230 Available at:
644 http://link.springer.com/10.1007/s002130050667.

645 Lewis DA, Melchitzky DS, Sesack SR, Whitehead RE, Auh S, Sampson A (2001) Dopamine
646 transporter immunoreactivity in monkey cerebral cortex: Regional, laminar, and
647 ultrastructural localization. J Comp Neurol 432:119–136.

648 Loewenfeld IE (1993) The pupil: anatomy, physiology, and clinical applications. Detroit:

Wayne State University.

Lovejoy LP, Krauzlis RJ (2010) Inactivation of primate superior colliculus impairs covert selection of signals for perceptual judgments. Nat Neurosci 13:261–266 Available at: http://www.nature.com/articles/nn.2470.

Maruff P, Hay D, Malone V, Currie J (1995) Asymmetries in the covert orienting of visual spatial attention in schizophrenia. Neuropsychologia 33:1205–1223.

McDougal DH, Gamlin PD (2014) Autonomic Control of the Eye. In: Comprehensive Physiology, pp 439–473. Hoboken, NJ, USA: John Wiley & Sons, Inc. Available at: http://doi.wiley.com/10.1002/cphy.c140014 [Accessed July 26, 2017].

McPeek RM, Keller EL (2002) Saccade target selection in the superior colliculus during a visual search task. J Neurophysiol 88:2019–2034 Available at: http://jn.physiology.org/content/88/4/2019%5Cnhttp://jn.physiology.org/content/88/4/2019.short%5Cnhttp://jn.physiology.org/content/jn/88/4/2019.full.pdf%5Cnhttp://www.ncbi.nlm.nih.gov/pubmed/12364525.

McPeek RM, Keller EL (2004) Deficits in saccade target selection after inactivation of superior colliculus. Nat Neurosci 7:757–763 Available at: http://www.nature.com/articles/nn1269.

Mehta MA, Owen AM, Sahakian BJ, Mavaddat N, Pickard JD, Robbins TW (2000) Methylphenidate Enhances Working Memory by Modulating Discrete Frontal and Parietal Lobe Regions in the Human Brain. J Neurosci 20:RC65–RC65 Available at: http://www.ncbi.nlm.nih.gov/pubmed/10704519.

Mitchell JF, Sundberg K a, Reynolds JH (2007) Differential Attention-Dependent Response Modulation across Cell Classes in Macaque Visual Area V4. Neuron 55:131–141

672 Available at: http://www.ncbi.nlm.nih.gov/pubmed/17610822 [Accessed November 25,
673 2014].

674 Mueller A, Krock RM, Shepard S, Moore T (2019) Dopamine Receptor Expression Among
675 Local and Visual Cortex-Projecting Frontal Eye Field Neurons. Cereb Cortex:1–17
676 Available at: https://academic.oup.com/cercor/advance-
677 article/doi/10.1093/cercor/bhz078/5481679.

678 Mueller A, Shepard SB, Moore T (2018) Differential Expression of Dopamine D5 Receptors
679 across Neuronal Subtypes in Macaque Frontal Eye Field. Front Neural Circuits.

680 Muller JR, Philiastides MG, Newsome WT (2005) Microstimulation of the superior
681 colliculus focuses attention without moving the eyes. Proc Natl Acad Sci 102:524–529
682 Available at: http://www.pnas.org/cgi/doi/10.1073/pnas.0408311101.

683 Mysore SP, Knudsen EI (2011) The role of a midbrain network in competitive stimulus
684 selection. Curr Opin Neurobiol 21:653–660 Available at:
685 http://linkinghub.elsevier.com/retrieve/pii/S0959438811000924.

686 Naber M, Alvarez GA, Nakayama K (2013) Tracking the allocation of attention using human
687 pupillary oscillations. Front Psychol.

688 Nelson CL, Sarter M, Bruno JP (2005) Prefrontal cortical modulation of acetylcholine release
689 in posterior parietal cortex. Neuroscience 132:347–359 Available at:
690 https://linkinghub.elsevier.com/retrieve/pii/S0306452205000229.

691 Newman DP, Cummins TDR, Tong JHS, Johnson BP, Pickering H, Fanning P, Wagner J,
692 Goodrich JTT, Hawi Z, Chambers CD, Bellgrove M a. (2014) Dopamine Transporter
693 Genotype Is Associated with a Lateralized Resistance to Distraction during Attention
694 Selection. J Neurosci 34:15743–15750 Available at:

695 http://www.jneurosci.org/cgi/doi/10.1523/JNEUROSCI.2327-14.2014 [Accessed
696 November 19, 2014].

697 Noudoost B, Moore T (2011a) Control of visual cortical signals by prefrontal dopamine.
698 Nature 474:372–375 Available at:
699 http://www.pubmedcentral.nih.gov/articlerender.fcgi?artid=3117113&tool=pmcentrez&
700 rendertype=abstract [Accessed October 10, 2014].

701 Noudoost B, Moore T (2011b) The role of neuromodulators in selective attention. Trends
702 Cogn Sci 15:585–591 Available at:
703 http://www.pubmedcentral.nih.gov/articlerender.fcgi?artid=3351278&tool=pmcentrez&
704 rendertype=abstract [Accessed October 15, 2014].

705 Ott T, Jacob SN, Nieder A (2014) Dopamine Receptors Differentially Enhance Rule Coding
706 in Primate Prefrontal Cortex Neurons. Neuron 84:1317–1328 Available at:
707 http://linkinghub.elsevier.com/retrieve/pii/S0896627314010125 [Accessed December 4,
708 2014].

709 Ott T, Nieder A (2016) Dopamine D2 Receptors Enhance Population Dynamics in Primate
710 Prefrontal Working Memory Circuits. Cereb Cortex:1–13 Available at:
711 http://cercor.oxfordjournals.org/cgi/doi/10.1093/cercor/bhw244.

712 Ott T, Nieder A (2019) Dopamine and Cognitive Control in Prefrontal Cortex. Trends Cogn
713 Sci 23:213–234 Available at: https://doi.org/10.1016/j.tics.2018.12.006.

714 Parikh V, Kozak R, Martinez V, Sarter M (2007) Prefrontal Acetylcholine Release Controls
715 Cue Detection on Multiple Timescales. Neuron 56:141–154 Available at: http://ac.els-
716 cdn.com/S0896627307006745/1-s2.0-S0896627307006745-main.pdf?_tid=c3c68606-
717 4baa-11e7-b903-
718 00000aab0f6b&acdnat=1496858425_98631c2399f8a1cfe667358952b60577 [Accessed

June 7, 2017].

Posner M (1990) The Attention System Of The Human Brain. Annu Rev Neurosci 13:25–42.

Robbins TW, Arnsten AFT (2009) The neuropsychopharmacology of fronto-executive function: monoaminergic modulation. Annu Rev Neurosci 32:267–287 Available at: http://www.pubmedcentral.nih.gov/articlerender.fcgi?artid=2863127&tool=pmcentrez&rendertype=abstract [Accessed July 20, 2014].

Sarter M, Hasselmo ME, Bruno JP, Givens B (2005) Unraveling the attentional functions of cortical cholinergic inputs: Interactions between signal-driven and cognitive modulation of signal detection. Brain Res Rev 48:98–111.

Sawaguchi T, Goldman-Rakic P (1991) D1 dopamine receptors in prefrontal cortex: involvement in working memory. Science (80- ) 251:947–950 Available at: http://www.ncbi.nlm.nih.gov/pubmed/1825731.

Sawaguchi T, Goldman-Rakic PS (1994) The role of D1-dopamine receptor in working memory: local injections of dopamine antagonists into the prefrontal cortex of rhesus monkeys performing an oculomotor delayed-response task. J Neurophysiol 71:515–528 Available at: http://www.physiology.org/doi/10.1152/jn.1994.71.2.515.

Sawaguchi T, Matsumura M, Kubota K (1990) Effects of dopamine antagonists on neuronal activity related to a delayed response task in monkey prefrontal cortex. J Neurophysiol 63:1401–1412 Available at: http://www.physiology.org/doi/10.1152/jn.1990.63.6.1401.

Seamans JK, Yang CR (2004) The principal features and mechanisms of dopamine modulation in the prefrontal cortex. Prog Neurobiol 74:1–58 Available at: http://www.ncbi.nlm.nih.gov/pubmed/15381316 [Accessed July 15, 2014].

Silk TJ, Newman DP, Eramudugolla R, Vance A, Bellgrove MA (2014) Influence of

742 methylphenidate on spatial attention asymmetry in adolescents with attention deficit
743 hyperactivity disorder (ADHD): Preliminary findings. Neuropsychologia 56:178–183.

744 Simonsohn U (2017) Two-Lines: A Valid Alternative to the Invalid Testing of U-Shaped
745 Relationships with Quadratic Regressions. Ssrn.

746 Soares D, Goldrick I, Lemon RN, Kraskov A, Greensmith L, Kalmar B (2017) Expression of
747 Kv3.1b potassium channel is widespread in macaque motor cortex pyramidal cells: A
748 histological comparison between rat and macaque. J Comp Neurol 525:2164–2174.

749 Soltani A, Noudoost B, Moore T (2013) Dissociable dopaminergic control of saccadic target
750 selection and its implications for reward modulation. Proc Natl Acad Sci U S A
751 110:3579–3584 Available at:
752 http://www.pubmedcentral.nih.gov/articlerender.fcgi?artid=3587234&tool=pmcentrez&
753 rendertype=abstract [Accessed December 29, 2014].

754 Thiele A, Bellgrove MA (2018) Neuromodulation of Attention. Neuron 97:769–785
755 Available at: https://doi.org/10.1016/j.neuron.2018.01.008 [Accessed February 27,
756 2018].

757 Thiele A, Brandt C, Dasilva M, Gotthardt S, Chicharro D, Panzeri S, Distler C (2016)
758 Attention Induced Gain Stabilization in Broad and Narrow-Spiking Cells in the Frontal
759 Eye-Field of Macaque Monkeys. J Neurosci 36:7601–7612 Available at:
760 http://www.ncbi.nlm.nih.gov/pubmed/27445139.

761 Thiele A, Delicato LS, Roberts MJ, Gieselmann MA (2006) A novel electrode-pipette design
762 for simultaneous recording of extracellular spikes and iontophoretic drug application in
763 awake behaving monkeys. J Neurosci Methods 158:207–211 Available at:
764 http://www.pubmedcentral.nih.gov/articlerender.fcgi?artid=2666830&tool=pmcentrez&
765 rendertype=abstract [Accessed November 18, 2014].

766 Thiele A, Herrero JL, Distler C, Hoffmann K-P (2012) Contribution of cholinergic and
767 GABAergic mechanisms to direction tuning, discriminability, response reliability, and
768 neuronal rate correlations in macaque middle temporal area. J Neurosci 32:16602–16615
769 Available at: http://www.ncbi.nlm.nih.gov/pubmed/23175816.

770 van Kempen J, Gieselmann MA, Boyd M, Steinmetz NA, Moore T, Engel T, Thiele A (2020)
771 Top-down coordination of local cortical state during selective attention.

772 Vigneswaran G, Kraskov A, Lemon RN (2011) Large Identified Pyramidal Cells in Macaque
773 Motor and Premotor Cortex Exhibit "Thin Spikes": Implications for Cell Type
774 Classification. J Neurosci 31:14235–14242.

775 Vijayraghavan S, Wang M, Birnbaum SG, Williams G V, Arnsten AFT (2007) Inverted-U
776 dopamine D1 receptor actions on prefrontal neurons engaged in working memory. Nat
777 Neurosci 10:376–384 Available at: http://www.ncbi.nlm.nih.gov/pubmed/17277774
778 [Accessed November 24, 2014].

779 Wang C-A, Boehnke SE, White BJ, Munoz DP (2012) Microstimulation of the Monkey
780 Superior Colliculus Induces Pupil Dilation Without Evoking Saccades. J Neurosci
781 32:3629–3636 Available at:
782 http://www.jneurosci.org/cgi/doi/10.1523/JNEUROSCI.5512-11.2012.

783 Wang C-A, Munoz DP (2015) A circuit for pupil orienting responses: implications for
784 cognitive modulation of pupil size. Curr Opin Neurobiol 33:134–140 Available at:
785 http://dx.doi.org/10.1016/j.conb.2015.03.018.

786 Warburton DM, Rusted JM (1993) Cholinergic control of cognitive resources.
787 Neuropsychobiology 28:43–46 Available at:
788 http://www.ncbi.nlm.nih.gov/pubmed/8255409.

Watanabe M, Kodama T, Hikosaka K (1997) Increase of Extracellular Dopamine in Primate Prefrontal Cortex During a Working Memory Task. J Neurophysiol 78:2795–2798 Available at: http://www.physiology.org/doi/10.1152/jn.1997.78.5.2795.

Williams G V, Goldman-Rakic PS (1995) Modulation of memory fields by dopamine D1 receptors in prefrontal cortex. Nature 376:572–575.

Zahrt J, Taylor JR, Mathew RG, Arnsten AFT (1997) Supranormal Stimulation of D 1 Dopamine Receptors in the Rodent Prefrontal Cortex Impairs Spatial Working Memory Performance. J Neurosci 17:8528–8535 Available at: http://www.jneurosci.org/lookup/doi/10.1523/JNEUROSCI.17-21-08528.1997.

# Figures

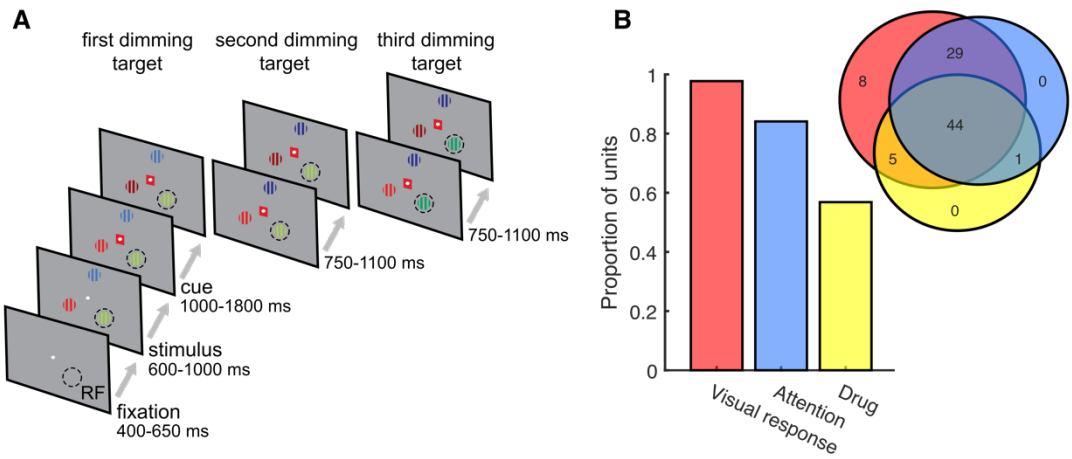


Figure 1. Experimental paradigm and unit selectivity. (**A**) Behavioral paradigm. The monkey held a lever and fixated on a central fixation spot to initiate the trial. One of 3 colored gratings was presented inside the receptive field (RF) of the neurons under study. After a variable delay a cue matching one of the grating colors surrounded the fixation spot, indicating which grating was behaviorally relevant (target). In pseudorandom order the stimuli decreased in luminance (dimmed). Upon dimming of the target, the monkey had to release the lever. (**B**) Proportion of units that are visually responsive, modulated by attention or drug application. Inset shows a Venn diagram of unit selectivity. Note that 1 unit was not selective for any of the experimental factors.

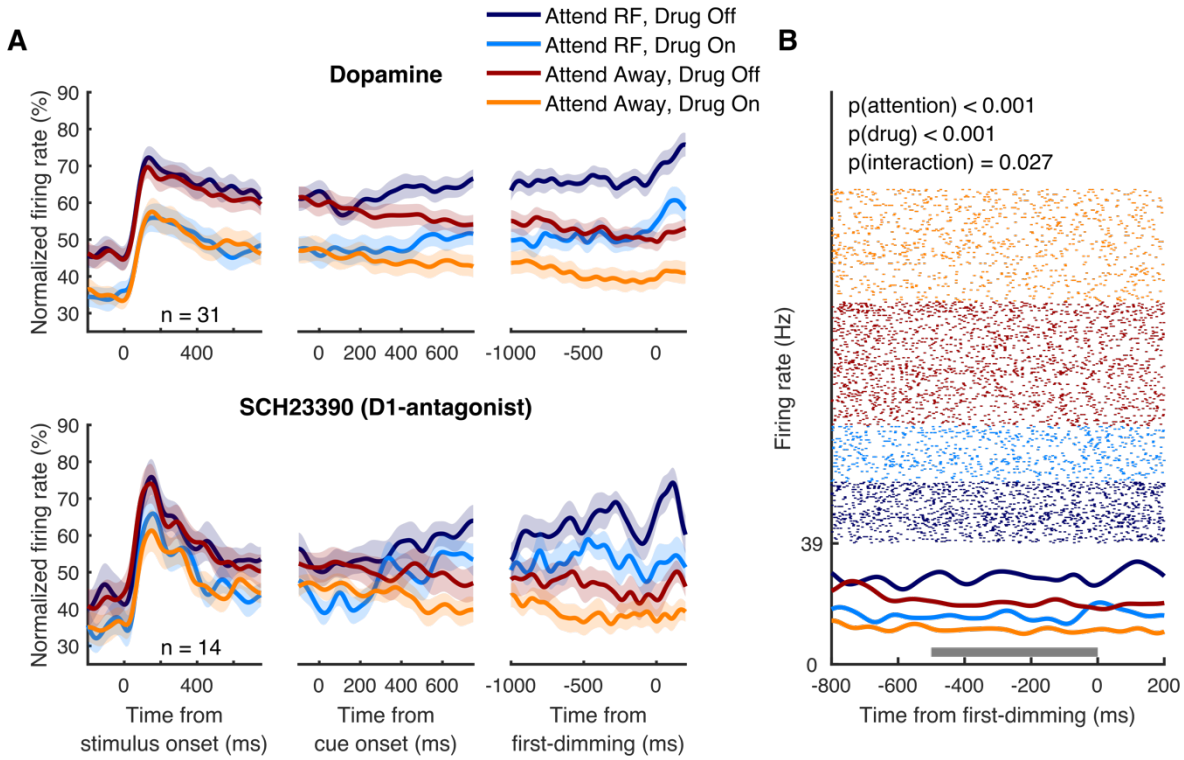


Figure 2. Population activity and example unit. (**A**) Population histograms for all cells recorded during dopaminergic drug application that were selective for attention and/or drug application. Population activity aligned to stimulus onset (left), cue onset (middle) and the first dimming event (right), for the non-specific agonist dopamine (top) and the D1 antagonist SCH23390 (bottom). Error bars denote ±1 SEM. (**B**) Activity from a representative cell recorded during application of the non-specific agonist dopamine.This cell's activity, aligned to the first dimming event, was significantly modulation by attention, drug application and showed a significant interaction between these factors. The grey bar indicates the time window used for statistical analyses. Statistics: two-factor ANVOVA.

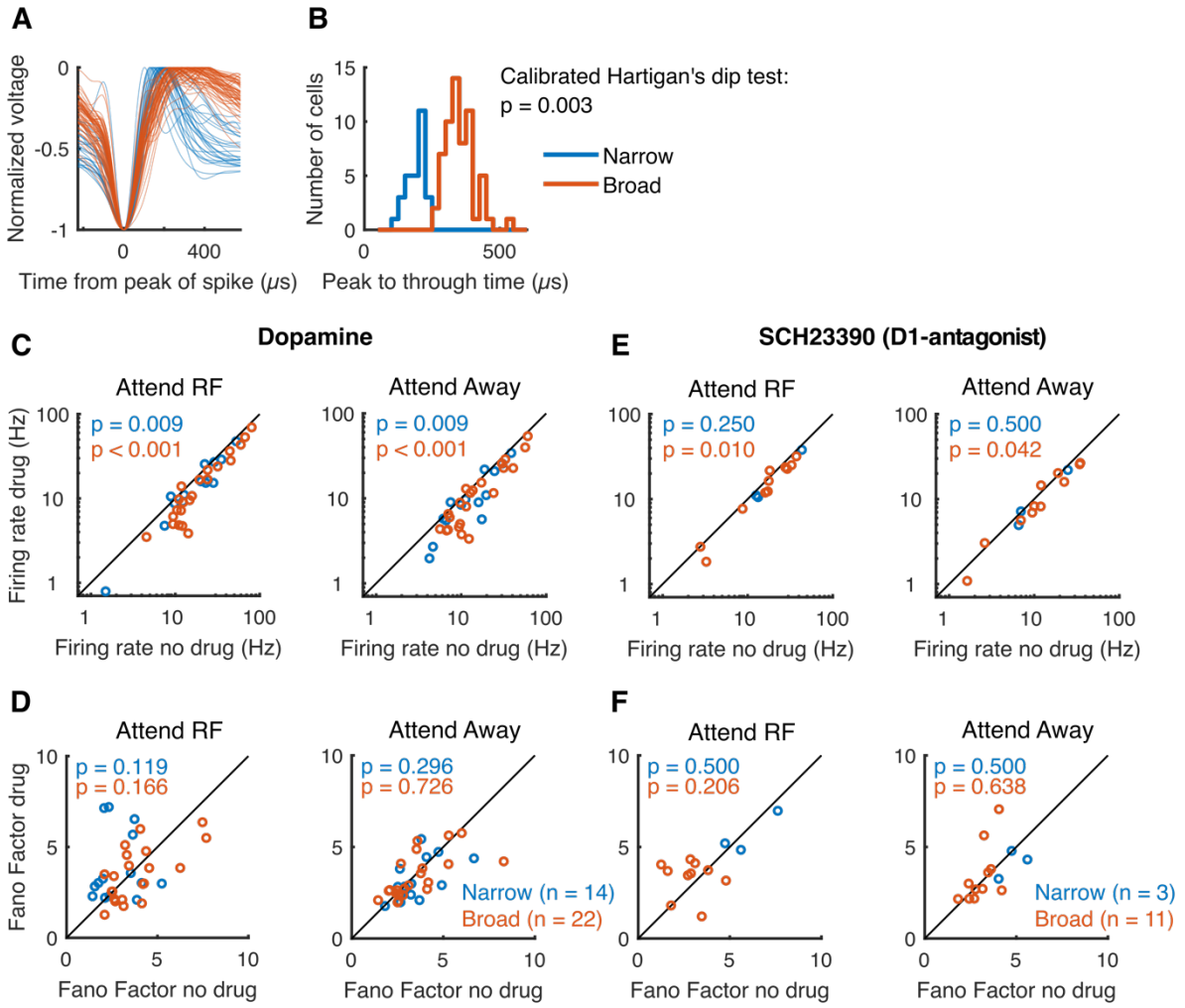


Figure 3. Dopaminergic modulation of firing rates across broad and narrow spiking units. (**A**) Average spike waveforms for the population of units. (**B**) Distribution of peak-to-trough ratios. Statistics: calibrated Hartigan's dip test (Ardid et al., 2015). (**C**) Average firing rates between no drug and drug conditions for the non-specific agonist dopamine for attend RF (left) and attend away (right) conditions. (**D**) Fano factors between no drug and drug conditions for the non-specific agonist dopamine. (**E-F** Same conventions as (**C-D**) but for the D1 antagonist SCH23390. Only units that revealed a main or interaction effect for the factor drug were included in this analysis. Statistics: two-sided Wilcoxon signed rank test.

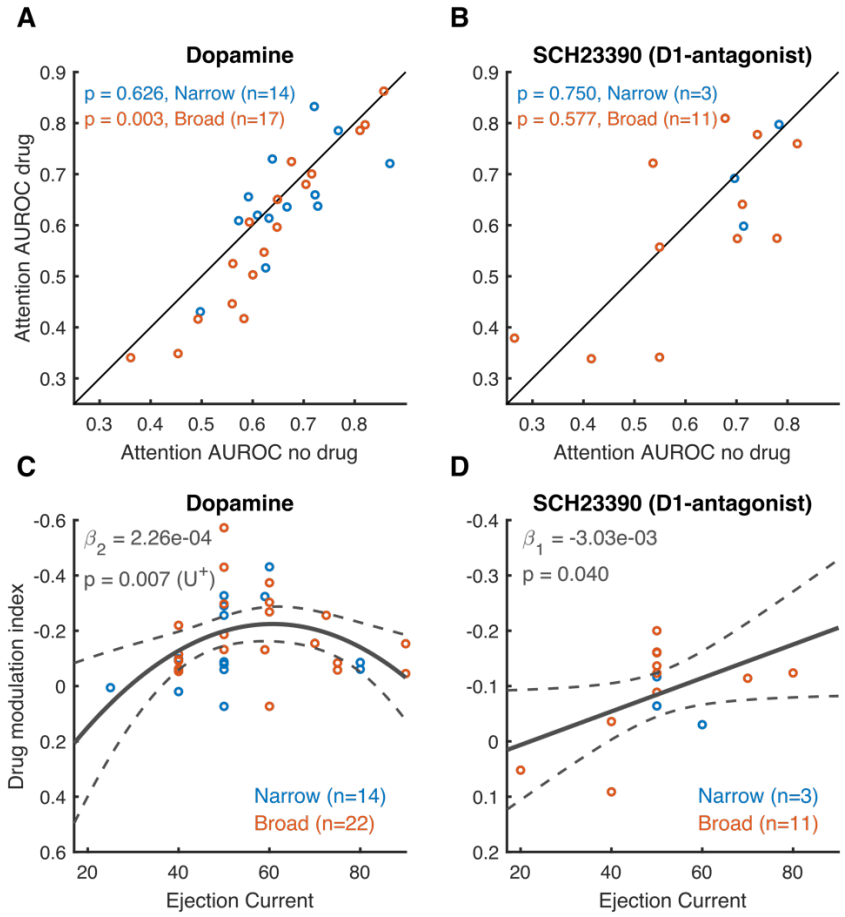


Figure 4. Dopaminergic modulation of AUROC values and dose-response curves. (**A**-**B**) Area under the receiver operating characteristic (AUROC) curve between no drug and drug conditions for the non-specific agonist dopamine (**A**) and the D1-receptor antagonist SCH23390 (**B**). Only cells that revealed a main or interaction effect for the factors drug and attention were included in this analysis. Statistics: Wilcoxon signed rank tests. (**C**-**D**) Drug modulation index plotted against ejection current for the non-specific agonist dopamine (**C**) and the D1 antagonist SCH23390 (**D**). Note the reversed y-axis. Solid and dotted lines represent significant model fits (applied to all cells simultaneously) and their 95% confidence intervals, respectively. A monotonic relationship is shown if a first-order fit was better than a constant fit, and a non-monotonic relationship is shown if a second-order fit was better than a linear fit. $U^+$ indicates a significant U-shaped relationship. Only cells that revealed a main or interaction effect for the factor drug were included in this analysis. Statistics: linear mixed-effects model analysis.

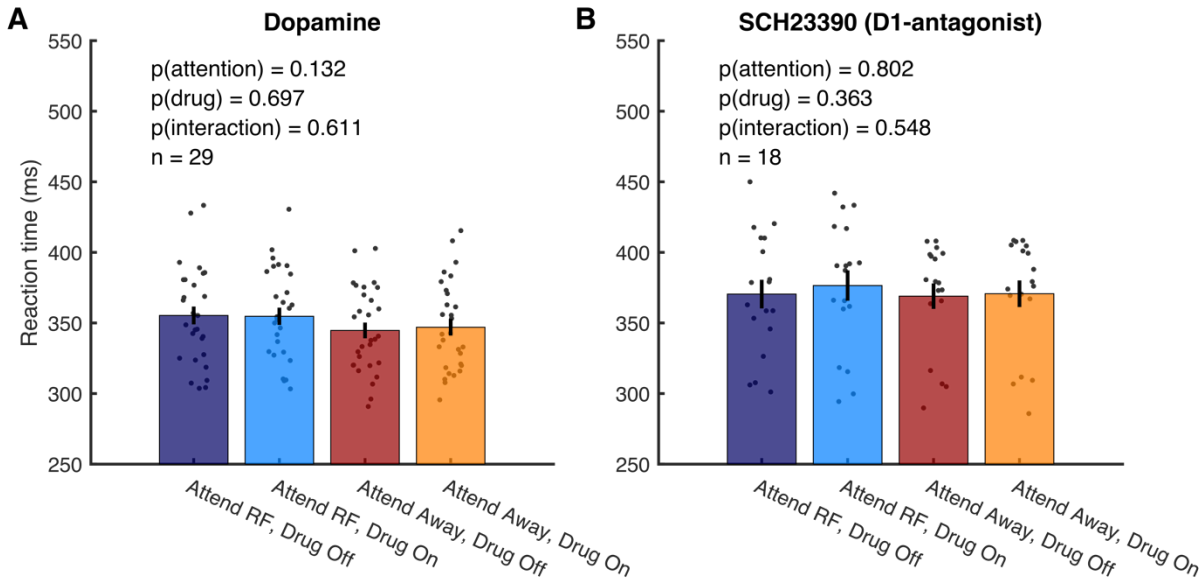


Figure 5. Behavioral performance is unaffected by iontophoretic application of dopaminergic drugs.Average RT on attend RF and attend away trials for the non-specific agonist dopamine (**A**) and the D1 antagonist SCH23390 (**B**). Dots represent average RT during a single recording session. Statistics: linear mixed-effects model analysis. Error bars denote ±1 SEM.

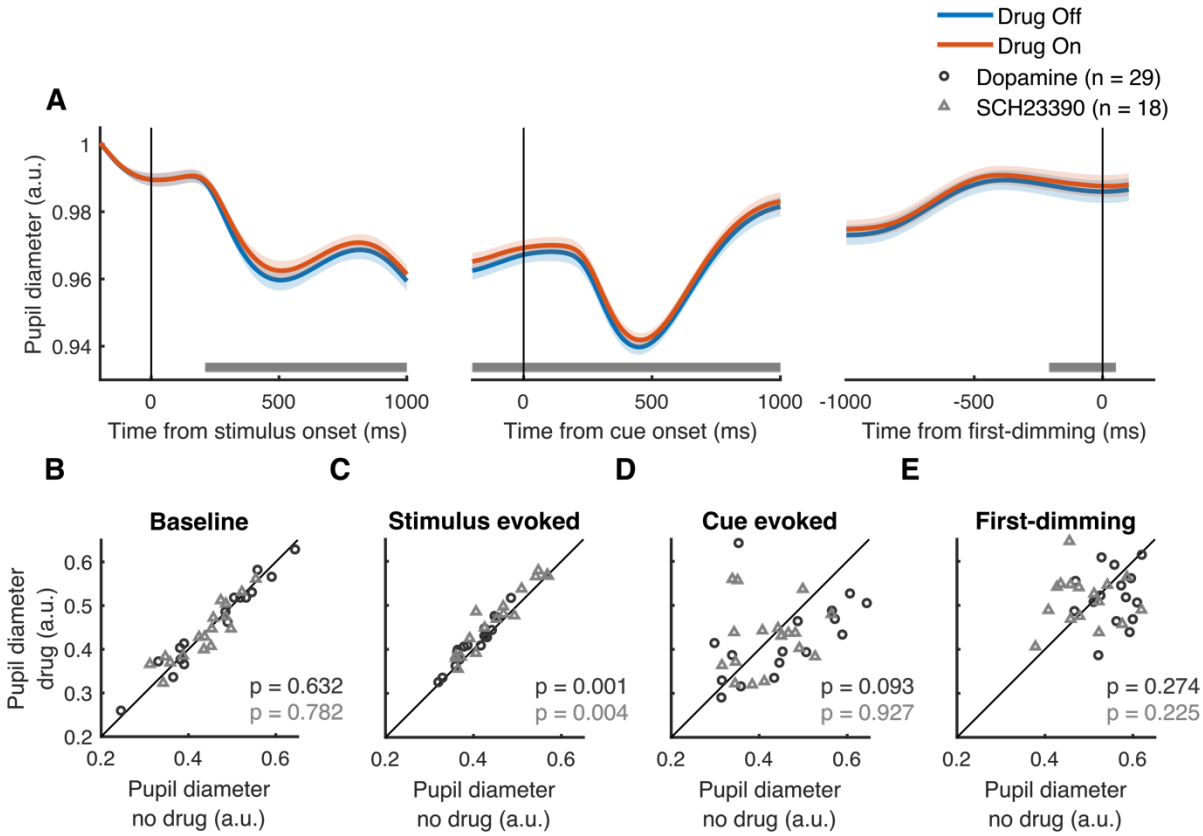


Figure 6. Modulation of pupil diameter by dopamine in Parietal cortex. (**A**) Baseline normalized pupil time course aligned to stimulus onset (left), cue onset (middle) and the first dimming event (right). The grey bar indicates the times where drug application brought about a significant difference in pupil diameter. (**B-E**) Average normalized pupil diameter during pre-stimulus baseline period (**B**), after stimulus onset, baseline corrected (**C**), after cue onset, corrected for pupil diameter before cue onset (**D**), and before the first dimming event, corrected for pupil diameter before cue onset (**E**). Shaded regions denote ±1 SEM. Statistics: Wilcoxon signed rank test. FDR correction was applied for the analysis in panel **A**.

# Tables

Table 1. Color values used for the 3 colored gratings across recording sessions and subjects, indicated as [RGB] – luminance (cd/m$^2$). a = Undimmed values, b = dimmed values.

| | ***Red*** | ***Green*** | ***Blue*** |
|---|---|---|---|
| ***Monkey 1***<br><br>***Early recordings (n=29)*** | a. [255 0 0] - 14.5<br><br>b. [100 0 0] - 1.4 | a. [0 128 0] – 9.1<br><br>b. [0 70 0] – 1.9 | a. [60 60 255] - 11.5<br><br>b. [10 10 140] – 2.2 |
| ***Monkey 2***<br><br>***Early recordings (n=5)*** | a. [220 0 0] – 12.8<br><br>b. [180 0 0] – 7.7 | a. [0 135 0] – 12.9<br><br>b. [0 110 0] – 7.3 | a. [60 60 255] – 12.2<br><br>b. [35 35 220] – 7.4 |
| ***Monkey 1/2 (n=12/8)***<br><br>***Late recordings*** | a. [220 0 0] – 12.8<br><br>b. [140 0 0] – 4.2 | a. [0 135 0] – 12.9<br><br>b. [0 90 0] – 4.6 | a. [60 60 255] – 12.2<br><br>b. [30 30 180] – 4.6 |